

This article may be downloaded for personal use only. Any other use requires prior permission of the author and AIP Publishing. This article appeared in C. A. Romero-Talamás, P. M. Bellan, S. C. Hsu; Multielement magnetic probe using commercial chip inductors. Rev. Sci. Instrum. 1 August 2004; 75 (8): 2664–2667. <https://doi.org/10.1063/1.1771483> and may be found at <https://pubs.aip.org/aip/rsi/article-abstract/75/8/2664/348220/Multielement-magnetic-probe-using-commercial-chip?redirectedFrom=fulltext>.

Access to this work was provided by the University of Maryland, Baltimore County (UMBC) ScholarWorks@UMBC digital repository on the Maryland Shared Open Access (MD-SOAR) platform.

Please provide feedback

Please support the ScholarWorks@UMBC repository by emailing scholarworks-group@umbc.edu and telling us what having access to this work means to you and why it's important to you. Thank you.

RESEARCH ARTICLE | AUGUST 03 2004

Multielement magnetic probe using commercial chip inductors

C. A. Romero-Talamás; P. M. Bellan; S. C. Hsu



Rev. Sci. Instrum. 75, 2664–2667 (2004)

<https://doi.org/10.1063/1.1771483>



CrossMark



APL Machine Learning

Latest Articles Online!

Read Now



Multielement magnetic probe using commercial chip inductors

C. A. Romero-Talamás, P. M. Bellan, and S. C. Hsu^{a)}

Applied Physics, Caltech, Pasadena, California 91125

(Received 2 January 2003; accepted 2 May 2004; published 3 August 2004)

A 60-element magnetic probe array has been constructed using miniature commercial chip inductors. The array consists of twenty clusters of three coils each mounted on a linear fixture. The coils are oriented in orthogonal directions to yield three-dimensional information. The array has been used to investigate magnetic properties of spheromaks. © 2004 American Institute of Physics. [DOI: 10.1063/1.1771483]

I. INTRODUCTION

Magnetic probes are widely used in measurements of current-carrying plasmas,^{1,2} but multielement and compact arrays are often difficult and tedious to make when winding coils manually.^{3–5} The part-to-part uniformity of hand-wound, millimetric size coils is usually poor since it is difficult to keep the wire aligned for every turn. Alignment and separation between coils can also become difficult if there is no substrate or fixture on which to mount the coils.

To give an idea of the difficulties in fabricating millimetric size coils, we compare the pick-up coils used in our probe, to those used in probes reported by Granetz *et al.*⁶ and Takahashi *et al.*⁷ Hand-winding 3 cm×8 mm coils with #30 AWG wire (as reported by Granetz *et al.*), is very different from hand-winding 2.9 mm×2.0 mm coils with a wire of size #42 (used in our probe). The diameter of a #30 wire is 0.254 mm, and the diameter of a #42 wire is 0.0635 mm, therefore the cross-sectional area of a #42 wire is 16 times smaller than that of a #30 wire and consequently the mechanical strength is also much smaller. Wire of #42 size can easily break if pulled too hard by hand. Takahashi *et al.* present a novel way of fabricating induction coils using thick-film technology. However the dimensions per coil that they used are too big (of the order of 1–2 cm) to create a multielement and compact array probe, especially if the probe is to be immersed in the bulk plasma.

The probe array presented here is designed for use in spheromak research, and has a combination of off-the-shelf components and custom computer-designed parts. The custom parts were machined to high precision with numerically controlled machine tools using information from computer-generated drawings. The coils are commercial chip inductors with precise dimensions and excellent consistency. The probe has a modular design for easy assembly and mounting on the chamber, and for easy component replacement if necessary.

Spheromaks⁸ are self-organizing, toroidal, axisymmetric magnetohydrodynamic configurations in which the magnetic fields are produced almost entirely by currents flowing in the

plasma. Although spheromak research is geared mainly to achieve the goal of thermonuclear fusion, spheromak physics is also relevant to the study of how plasma magnetic topology evolves.

At Caltech, spheromaks are created in a large cylindrical vacuum chamber using a planar gun⁹ (see Fig. 1). Since spheromaks in the Caltech chamber expand freely and translate away from the gun, a magnetic probe can be fixed in front of the gun; the recorded signals can then be combined to produce contour maps of the spheromak as it flows past the probe.¹⁰

II. DESIGN AND CONSTRUCTION

Sixty commercial chip inductors with 52 turns each (inductance=5±0.1 μH) were used (Coilcraft Inc., model 1008CS-472XGGB). The nominal dimensions of the chip inductors are 2.8 mm×2.9 mm×2.0 mm. The inductors were inserted into a Delrin plastic retention fixture that was fabricated to precise specifications using numerically controlled machining (see Fig. 2). The spacing between clusters is 20 mm; thus the effective probe length is 380 mm.

Pairs of twisted magnet wires (38-gauge) were soldered to the terminals of the inductors. Each twisted pair of wires connects to a BNC panel jack, and the signal of each coil is recorded using 100 MHz, 12-bit analog to digital converters (ADC). The soldering of the wires was done manually using a precision jig made to hold the wires in place on top of each terminal during the soldering operation. A special grinding machine (Carpenter Mfg. Co., model 88-D) was used to strip the insulation enamel from the wires.

Teflon tape was wrapped around the subassembly of the plastic fixture, chip inductors and magnet wires to prevent damage during the insertion of the assembly into its housing. The housing was made of quartz tubing to prevent electrical interaction with the plasma. The coils, plastic fixture, and wiring remain at atmospheric pressure, since the housing is vacuum tight. The probe diameter is 8.4 mm.

To connect the quartz tube to the rest of the housing, Torr-seal vacuum epoxy was used to fix the quartz tube to a standard Swagelok VCO socket gland. A tight fit of the plastic fixture into a Swagelok elbow prevents the subassembly from rotating after assembling the probe and tightening the vacuum seals. The coil cables were soldered to three

^{a)}Current address: P-24 Plasma Physics Group, Los Alamos National Laboratory, Los Alamos, NM 87545.

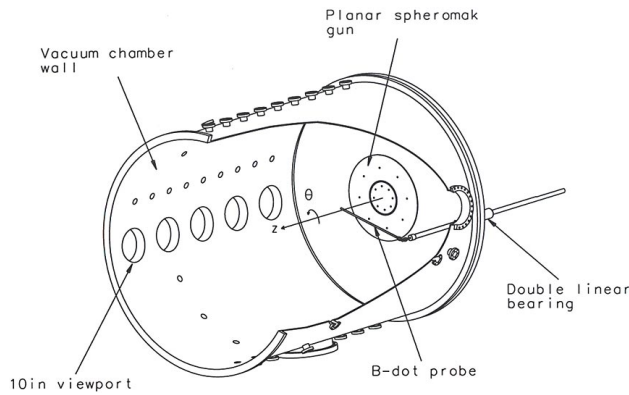


FIG. 1. (Color online) Cutaway view of Caltech vacuum chamber. Magnetic probe (labeled B-dot) is placed in front of planar spheromak gun. The spheromak gun is 50.8 cm in diameter, and the chamber dome is 137 cm in diameter.

20×2 -pin insulation displacement connector sockets (3M, model 517-89140-0001), which were then inserted into a metal box that serves as an EMI shield and panel for the BNC connectors.

The mechanical support of the probe is achieved through a 1 in. diameter, highly polished stainless steel tube. The tube is connected to the probe housing through a combination of standard Swagelok connectors and custom-made welded reducers. Once mounted on the vacuum chamber, the probe can slide in the Z direction and also rotate in the θ direction. The vacuum seal is achieved by an O-ring seal around the 1 in. diameter tubing, mounted on a 2.75 in. flange. A high-precision, double linear bearing (McMaster-Carr, model 64825K87) mounted on the outside of the chamber assures that the 1 in. diameter tubing remains parallel to the Z direction (see Fig. 3). The double linear bearing also relieves the O-ring seal from any load that could result from the weight of the probe and the 1 in. diameter tube. Even though the entire probe assembly is very rigid, care was taken to ensure that the probe position would not be affected by deflection or sagging from the weight of the tubing or its connectors. Positioning measurements were carried out for the 50 cm range of motion required in our experiments. Positioning in the θ direction was measured with a tilt indicator

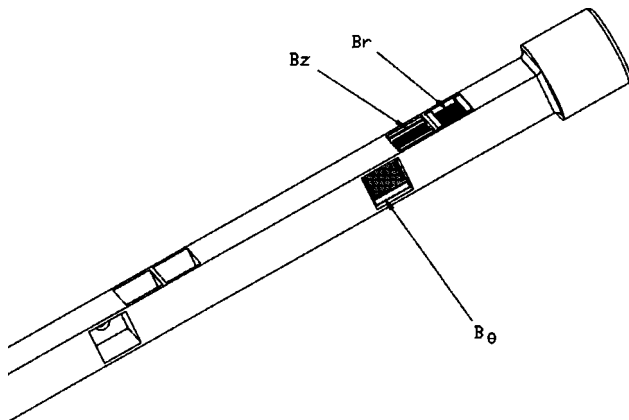


FIG. 2. Plastic retention fixture for induction coils. Two clusters are shown. The cluster on the right contains the inductor coils, with the direction of the B field that they measure indicated.

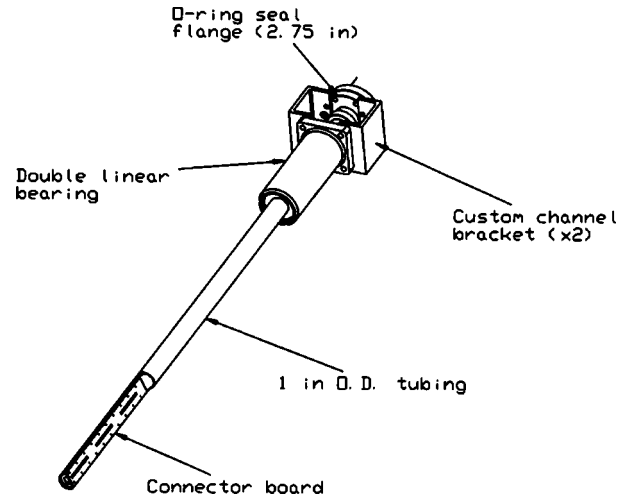


FIG. 3. External view of the magnetic probe mounted on the Caltech vacuum chamber. The 2.75 in. O-ring seal flange is attached to the vacuum chamber flange. Note: Probe connectors and EMI shield not shown.

attached to the 1 in. diameter tubing at the outside of the vacuum chamber. In a 50 cm displacement range no deflection was detected, to within 1 mm precision in the positioning of the probe. All measurements were carried out with respect to the axis of the planar spheromak gun shown in Fig. 1. Fiducial marks were placed on the tubing to facilitate alignment when moving the probe between experimental runs.

III. OPERATION PRINCIPLE AND CALIBRATION

Using Faraday's law, the induced voltage in a loop of conducting material in the presence of a time-varying magnetic field is $V = -d\Phi/dt$, where Φ is the magnetic flux through the loop. If every coil has N turns with an area A , the induced voltage can be expressed as $V = -NA(dB/dt)$. For practical purposes, the values N and A can be lumped into one constant, which we will refer to as the NA value.

To obtain the NA value for every coil, a Helmholtz coil was used to produce a known magnetic field. Since the current through the Helmholtz coil is known, the expression for calibration becomes

$$NA = \frac{a \int_{t_0}^t V_{\text{coil}}(t') dt'}{\left(\frac{4}{5}\right)^{3/2} \mu_0 n [I(t')]_{t_0}^t}, \quad (1)$$

where a , $I(t')$, and n are, respectively, the Helmholtz coil radius, current, and number of turns, and $V_{\text{coil}}(t')$ is the voltage across the terminals of the pick-up coil.

For every cluster of coils, a calibration operator was defined for precise measurements, since it is possible that a given coil can pick up unwanted signal (i.e., different from the intended direction) at the interface between the soldered wire and the coil. The calibration operator subtracts the unwanted signals and is defined as follows:

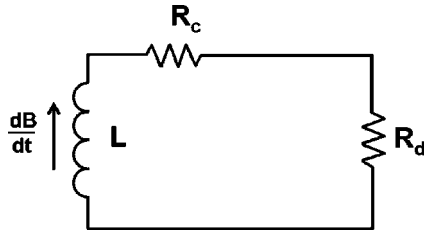


FIG. 4. Equivalent circuit for each coil in the magnetic probe, including the transmission line to the digitizer. Measured values are $L=6.17 \mu\text{H}$, $R_c=12\Omega$, and $R_d=50\Omega$.

$$\mathbf{C} = \begin{pmatrix} 1 & -C_{R\theta} & -C_{RZ} \\ -C_{\theta R} & 1 & -C_{\theta Z} \\ -C_{ZR} & -C_{Z\theta} & 1 \end{pmatrix} \quad (2)$$

with the components of the operator defined as

$$C_{ij} = \frac{NA_i^{\text{perp}}}{NA_i} \quad (3)$$

with NA^{perp} being the NA value for the pick-up of a signal by a coil oriented perpendicular to the direction being measured (also the direction of the \mathbf{B} field). The true field is then

$$\mathbf{B} = \mathbf{C} \cdot \mathbf{B}_m, \quad (4)$$

where $\mathbf{B}_{m_i} = -1/NA_i \int_{t_0}^t V_i(t') dt'$.

The average value for the effective NA was found to be $1.21 \times 10^{-4} \text{ m}^2$ for the probe presented here. All the coils

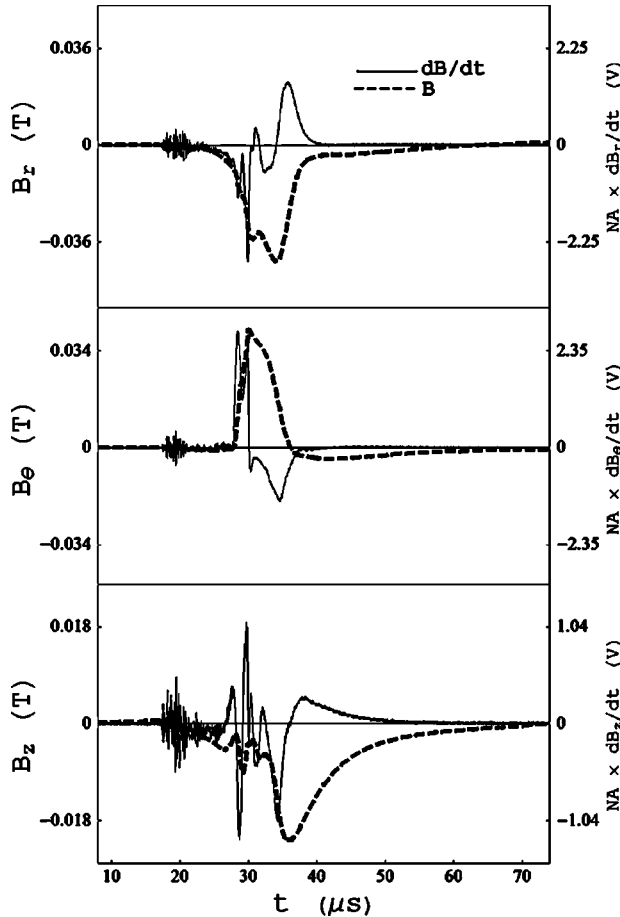


FIG. 5. Digitizer and integrated signals of the cluster found at $R=12 \text{ cm}$.

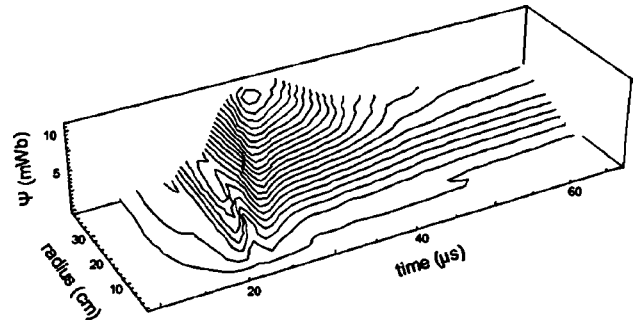


FIG. 6. Contours of constant ψ (in units of mWb). Contours are drawn along the vertical axis every 0.5 mWb. The top (closed) contour represents 10.6 mWb. The probe was placed 22.5 cm away from the planar gun. Shot #4855.

were absolutely calibrated in the probe assembly using a pulsed capacitor bank power supply that rings at 280 kHz. The relative uncertainty of the calibration system, including the power supply for the Helmholtz coil and the digitizers was 0.48%. The average absolute value for the off-diagonal elements of the calibration operator was found to be 0.076.

The relative difference of NA values between clusters was found to be 2.4% for the R -direction coils and 4.3% for the θ - and Z -direction coils. The main reason for such variation in the θ - and Z -direction coils is the small wire loop that results at the interface of each coil and its leads. Given the thin wire used, it was difficult to twist the wire tightly at the interface with the chip inductor without breaking the wire. In the R direction the variation comes mainly from the inductance tolerance of the commercial chip inductors used.

The phase shift between the known magnetic field signal and the probe signal at the digitizers was also measured during calibration. The difference in phase between the two signals yielded a time lag in the probe current of $114 \pm 17 \text{ ns}$. The electrical circuit for any given coil in the probe and its corresponding digitizer channel is shown in Fig. 4. The equation for the coil current is

$$L \frac{dI}{dt} + I(R_d + R_c) = \phi_0 \cos(\omega t), \quad (5)$$

where R_d is the digitizer and cable impedance (50Ω), R_c is the coil and coil lead resistance (12Ω), L is the inductance of the coil, and I is the current through the circuit. The right-hand side represents the voltage source due to the time-dependent flux linked by the coil. This flux is due to the external magnetic field, $B \times NA$. The solution for the above equation can be written as

$$I(t) = \frac{\phi_0}{\sqrt{(R_d + R_c)^2 + \omega^2 L^2}} \cos(\omega t - \theta) \quad (6)$$

with $\theta = \tan^{-1}(\omega L / (R_d + R_c))$ being the phase shift. For the values shown in Fig. 4, $\theta = 0.173 \text{ rad}$, or equivalently a time lag in the signal of $\Delta t = 99 \text{ ns}$ is obtained.

IV. MEASUREMENTS

Figure 5 shows an example of the raw signal (dB/dt) and integrated signal (B) at a radius of 12 cm from the axis

of the chamber (see Fig. 1). The sampling time for the raw data is $0.01\ \mu\text{s}$, and the integration was performed numerically.¹¹

Using the Single Shot Propagation Inference (SSPI) method described by Yee and Bellan,¹⁰ it is possible to obtain approximate information on magnetic topology from a single discharge. Figure 6 shows a contour plot of data from the entire magnetic probe array; the contours represent surfaces of constant magnetic flux, $\psi(r, z_p) = \int_0^r 2\pi r' B_z(r', z_p) dr'$, where z_p is the axial coordinate in the frame of reference of the plasma. The propagation velocity of the plasma was estimated to be $V_p = 1.5\ \text{cm}/\mu\text{s}$ from images taken with a 16-frame, gated, intensified CCD camera (DRS Hadland Imacon 200). The probe was placed at $z = 22.5\ \text{cm}$ from the planar gun ($z = 0$). Assuming constant V_p and using the transformation $z_p = z - V_p t$, we find that the range of time shown in Fig. 6, $10\ \mu\text{s}$ to $65\ \mu\text{s}$, corresponds to $97.5\ \text{cm}$ to $15\ \text{cm}$ (note that the direction of the distance axis reverses with respect to the direction of the time axis). Thus, the time axis in Fig. 6 can be transformed to a distance axis to obtain spatial information of the magnetic flux along the Z direction.

ACKNOWLEDGMENTS

The authors would like to thank Dave Felt, Ricardo Paniagua, and Larry Begay for their contributions to the construction of the magnetic probe, and to Eli Jorne and Setthivoine You for their contributions during the calibration process. This work was supported by U.S. DOE Grant No. DE-FGO3-98ER544611.

¹R. H. Lovberg, in *Plasma Diagnostic Techniques*, edited by R. H. Huddleston and S. L. Leonard (Academic, New York, 1965), Chap. 3.

²I. H. Hutchinson, *Principles of Plasma Diagnostics* (Cambridge University Press, Cambridge, 1987), Chap. 2.

³D. E. T. F. Ashby, L. S. Holmes, and M. A. Kasha, *J. Sci. Instrum.* **40**, 364 (1963).

⁴P. Beiersdorfer and E. J. Clothiaux, *Am. J. Phys.* **51**, 1031 (1983).

⁵D. G. Pellinen *et al.*, *Rev. Sci. Instrum.* **51**, 1535 (1980).

⁶R. S. Granetz *et al.*, *Rev. Sci. Instrum.* **61**, 2967 (1990).

⁷H. Takahashi *et al.*, *Rev. Sci. Instrum.* **72**, 3249 (2001).

⁸P. M. Bellan, *Spheromaks: A Practical Application of Magnetohydrodynamic Dynamos and Plasma Self-organization* (Imperial College Press, London, 2000).

⁹S. C. Hsu and P. M. Bellan, *Mon. Not. R. Astron. Soc.* **334**, 257 (2002).

¹⁰J. Yee and P. M. Bellan, *Phys. Plasmas* **7**, 3625 (2000).

¹¹S. Wolfram, *The Mathematica Book*, 4th ed. (Cambridge University Press and Wolfram Media, New York, 1999), pp. 909–916.